A Methodology to Model the Statistical Fracture Behavior of Acrylic Glasses for Stochastic Simulation

Marcel Berlinger[1]
Stefan Kolling[1]
Andreas Rühl[1]
Jens Schneider[2]
[1]*Institute of Mechanics and Materials*
Technische Hochschule Mittelhessen
Wiesenstraße 14, Giessen 35390, Germany
[2]*Technical University of Darmstadt*
Institute for Structural Mechanics and Design
Franziska-Braun-Strasse 3, Darmstadt 64287, Germany

Abstract

*Acrylic glass made of PMMA bears great potential for automotive glazing. As a substitute for mineral glass, new freeform designs become possible with a simultaneous reduction of the structural weight. Under safety aspects of highly weight optimized components, a very precise knowledge of the material behavior is necessary since it is well known that PMMA is a material with high variability in its strength. In the present work, a methodology is proposed to determine the statistical probability distribution of fracture strains from experimental testing. Subsequently, a rate-dependent stochastic failure model is developed. By generation of uniformly distributed random numbers which represent the occurrence probability, *MAT_ADD_EROSION cards for LS-DYNA® are used, containing the tabulated fracture strains at different strain-rates. For stochastic simulation there are two possible procedures to apply the present model. The user provides a distinct probability quantile, e.g. 5 % occurrence probability, generates the corresponding *MAT_ADD_EROSION card and performs a worst-case simulation. Alternatively, the user generates a random set of probability quantiles, i.e. N values from zero to one, and performs N simulations. As an application, the last procedure is used in order to show the influence of a varying fracture strain on the head injury criterion (HIC) in validation tests on PMMA side windows. The example demonstrates the necessity of stochastic simulation for a reliable quantification of injury criteria in crashworthiness analysis.*

Introduction

Like mineral glass, acrylic glass behaves highly stochastic due to its strain at failure. That complicates a predictive simulation of structural parts, which is usually based on pretended deterministic values. In this work, the results of the preliminary studies from RÜHl [1] are utilized to describe the viscoelastic stress-strain behaviour of the material for numerical simulation with LS-DYNA. Using *MAT_GENERAL_VISCOELASTIC (*MAT_76), it was possible to predict the initial rate-dependent stiffness of the material. In Figure 1 the simulation model is compared to experimental tensile tests at various load velocities. By using a linear visco-elastic material law there is an unavoidable deviation at higher strains where nonlinearity becomes an issue. As indicated in Figure 1 the hitherto existing simulation model features a distinct fracture strain from averaging experimental results. In the following a statistical model is presented in order to introduce a stochastic failure criterion.

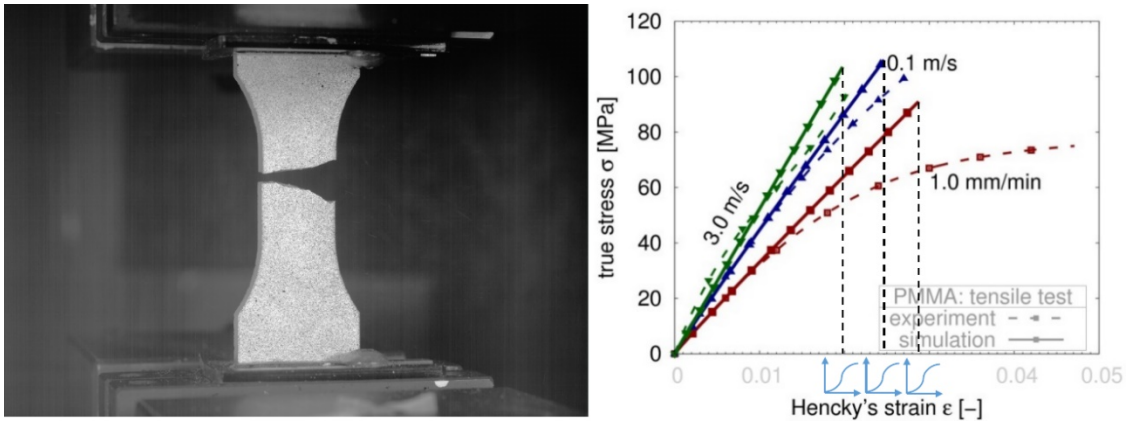

Figure 1 - Modeling of the tensile test with distinct failure criterion instead of a stochastic fracture.

The necessity for such a failure criterion is illustrated in the comparison of the simulation model from [2] to further load cases as in Figure 2, where the acrylic glass is tested under bending load. The wide spread of the fracture strain clearly shows the insufficiency of a distinct failure value. Likewise, the dart test shown in Figure 3, see [3], illustrates the same behaviour.

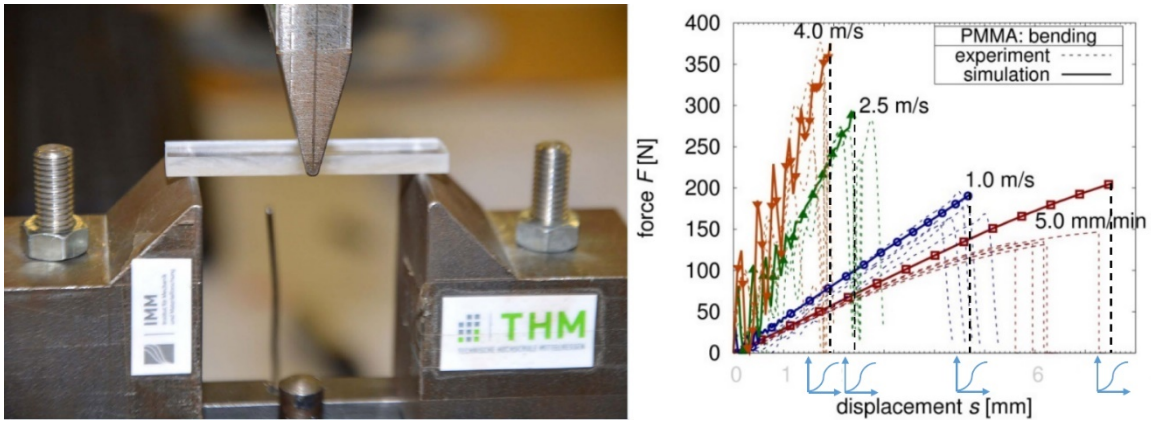

Figure 2 - Modeling of the 3-point bending test with distinct failure criterion instead of a stochastic fracture.

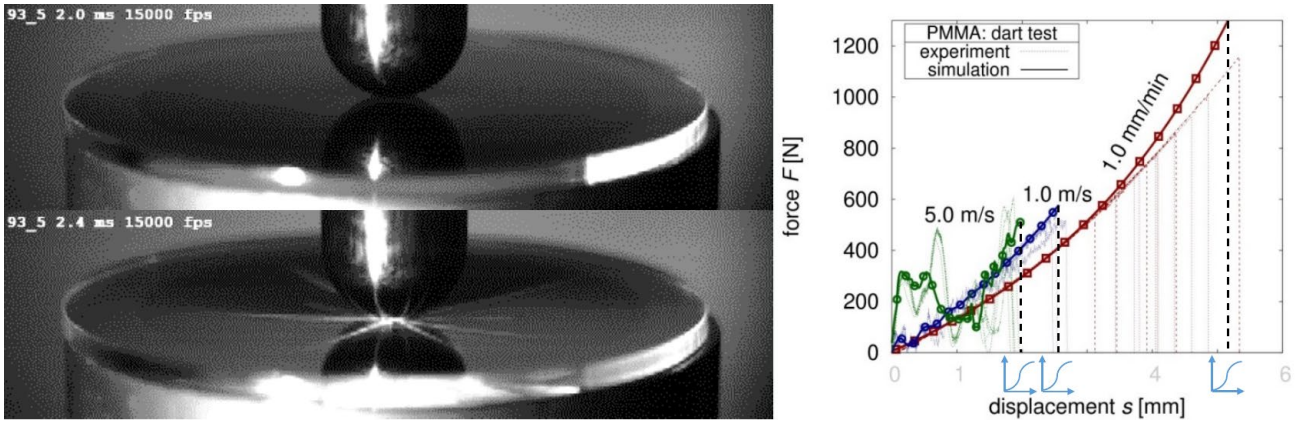

Figure 3 - Modeling of the dart test with distinct failure criterion instead of a stochastic fracture.

For validation of the *MAT_GENERAL_VISCOELASTIC card, head impact tests were realized experimentally using automotive rear side windows. An extensive study with different Plexiglas® materials is given by [4]. An image series of this test is shown in Figure 4.

Figure 4 - Head impact test on side window for validation

As usual in pedestrian protection, the measured quantity is the resultant acceleration in the center of gravity of the head impactor over time. Due to the rear side windows comparatively small size a child head-form impactor is applied. Note that this test setupt is used for validation only and does not follow any crash test regulation. The impact of the dummy head on a defined point on the screen occurs with a velocity of 10 m/s. Here, the side window itself is made of monolithic PMMA with 4 mm thickness.

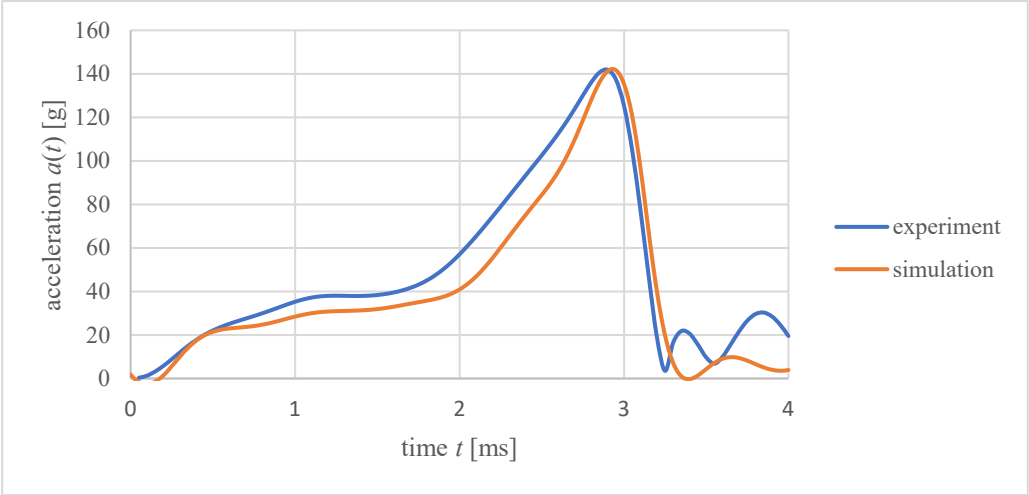

Figure 5 - Resultant acceleration of the head impactor

In a reverse engineering process the failure strain is determined for the best reproduction of the impactor's acceleration. In Figure 5 the resultant acceleration is shown filtered by SAE J211 CFC 1000 as it is common practice for head impact tests. Again, this is only a deterministic failure criterion. So, in order to show the influence of a varying fracture strain, the simulation model is supplemented by a statistical approach and based on the head impact tests the head injury criterion is examined.

Experimental Research

For statistical analyses on the fracture behaviour of PMMA sufficient sample sizes are necessary. Uniaxial tensile tests were performed at seven different loading velocities. Analogous to [1] the dimensions of the BZ tensile specimen are adopted, see Figure 6. This geometry is optimized for putting comparatively high strain rates on the measuring zone at adequate haul-off speed of the testing machine. The level of triaxiality *m,* Equation (1), in the measuring zone and towards the edges is nearly 1/3, i.e. uniaxial stress is ensured, see Figure 6. Hereby, the triaxiality is the relation of hydrostatic pressure p over von Mises stress σ_{vM}:

$$m = -\frac{p}{\sigma_{vM}} = \frac{\frac{1}{3}(\sigma_1+\sigma_2+\sigma_3)}{\sqrt{\frac{1}{2}[(\sigma_1-\sigma_2)^2+(\sigma_2-\sigma_3)^2+(\sigma_3-\sigma_1)^2]}}. \quad (1)$$

For the local strain at failure, the surface strain is measured via digital image correlation (DIC). For the quasi-static velocity, a 3D camera system and for the higher strain rates a 2D highspeed camera has been used. The different test setups are summarized in Table 1. The fracture strain is taken at the position of crack initiation one picture before failure, as shown in Figure 6.

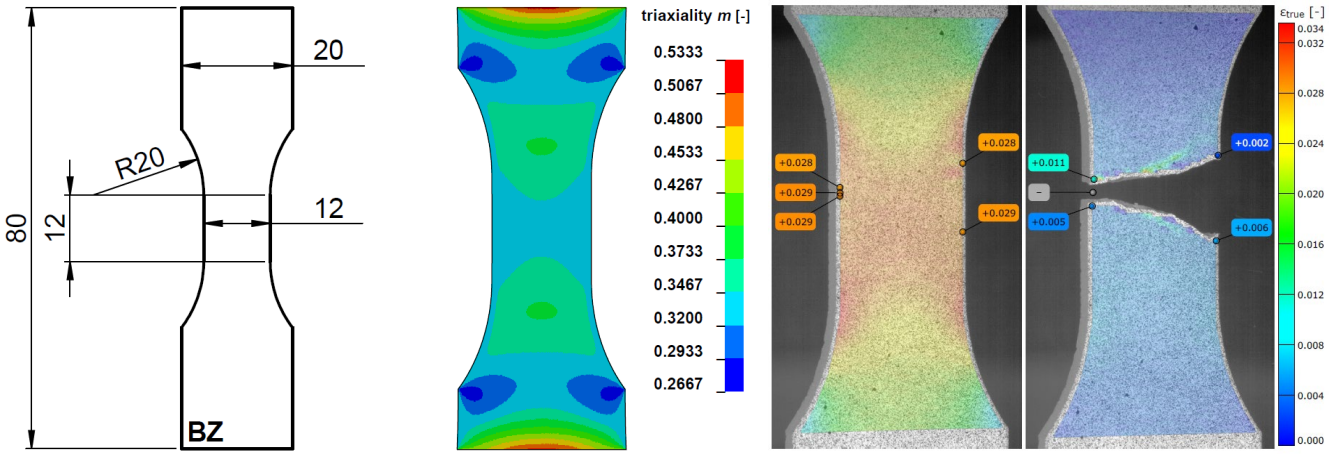

Figure 6 – Dimensions of the BZ tensile specimen, level of triaxiality, and local strain measurement via DIC

Six of seven haul-off speeds are performed on common material testing machines, one electro-mechanical, and one servo-hydraulic. The highest velocity is realized in a drop tower system, as shown in Figure 7. A weighted striker drops from defined height to catch the lower clamping of the specimen at a speed of 3 m/s. The upper clamping is fixed to a force sensor. Again, a highspeed camera films the specimen's surface during deformation.

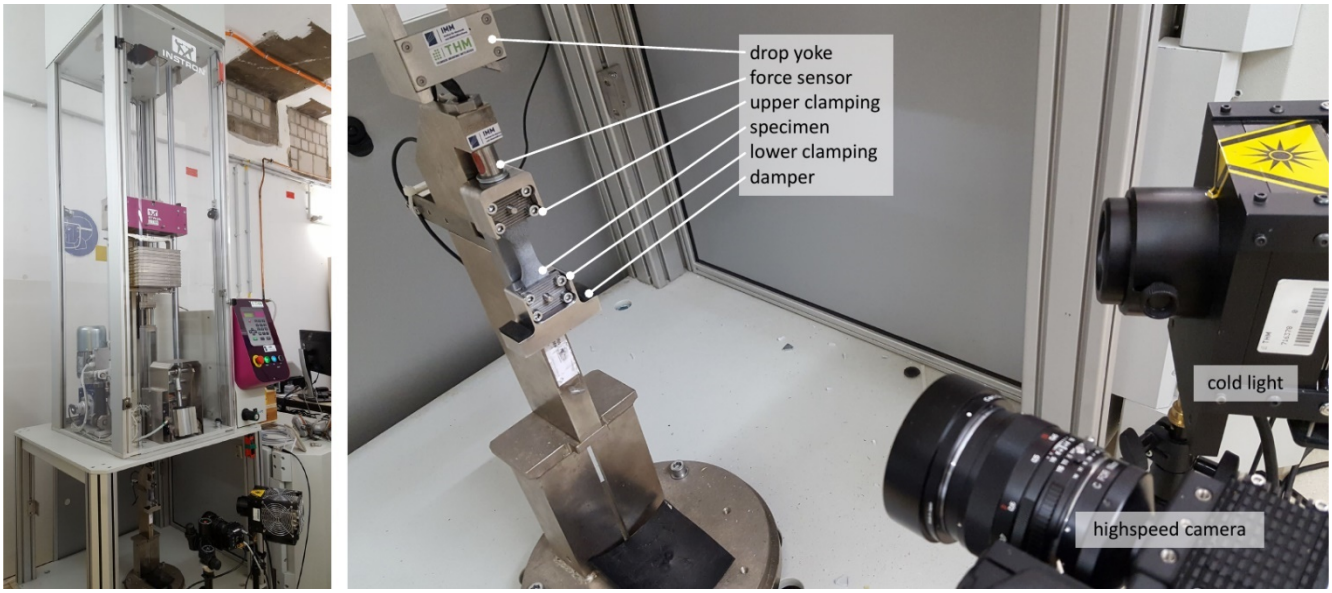

Figure 7 – Drop tower test setup for realization of higher strain rates.

Table 1 – Realized strain rates with the different test setups

Reference	Strain Rate [1/s]	Testing Machine	DIC system
$\dot{\varepsilon}_1$	4.6 E+1	drop-tower system	2D highspeed camera
$\dot{\varepsilon}_2$	3.8 E +0	servo-hydraulic system	2D highspeed camera
$\dot{\varepsilon}_3$	9.7 E -1	servo-hydraulic system	2D highspeed camera
$\dot{\varepsilon}_4$	1.6 E -1	servo-hydraulic system	2D highspeed camera
$\dot{\varepsilon}_5$	2.0 E -2	servo-hydraulic system	2D highspeed camera
$\dot{\varepsilon}_6$	2.0 E -3	electro-mechanical system	2D highspeed camera
$\dot{\varepsilon}_7$	1.6 E -4	electro-mechanical system	3D dual camera

In sum, over 360 tensile tests are conducted with at least 50 repetitions per haul-off speed. The aim is to hold minimum 30 valid tests for the stochastic analyses, because it showed that the fitted probability distribution function is stable in its function parameters for this number of samples.

Statistical Modeling

At this point, we begin with seven sets of experimental fracture strains from the seven haul-off speeds. So far, there is no information of the probability for each fracture strain. Therefore, one of the so-called probability estimators is used [5]. For each set the fracture strain are sorted in ascending order, i.e. $\varepsilon_1 \leq \varepsilon_2 \leq \cdots \leq \varepsilon_n$. Dependent on their position in the ordering, the occurrence probability is then assigned by

$$p_i = \frac{i}{n+1}, \tag{2}$$

which is referred to as Weibull's probability estimator [6] and well proven [7]. Upon these coordinates $(\varepsilon_i|p_i)$, a respective probability distribution function is fitted. The two-parameter Weibull distribution showed the best reproduction of the empirical data. Its cumulative distribution function (CDF) is given as

$$P(\varepsilon) = 1 - \exp\left[-\left(\frac{\varepsilon}{\eta}\right)^{\beta}\right]. \tag{3}$$

The function fit is realized by optimization of the parameters for the least deviation to the empirical data, as minimization of a weighted residual sum of squares

$$WRSS = \sum_{i=1}^{n}\left\{[p_i - P(\varepsilon_i)]^2 \cdot \frac{1}{P(\varepsilon_i)[1-P(\varepsilon_i)]}\right\}. \tag{4}$$

The included weighting factor, which is adopted from [8], puts higher weight to the function tails, meaning that the strains of beginning fracture and those of maximum are captured better. Alternative fit approaches are given by [9]. The seven determined two-parameter Weibull distributions are depicted in Figure 8. They clearly show a decreasing level of the fracture strain with increasing strain rate. Simultaneously, the spreading, i.e. the width of the fracture strains interval, is reduced.

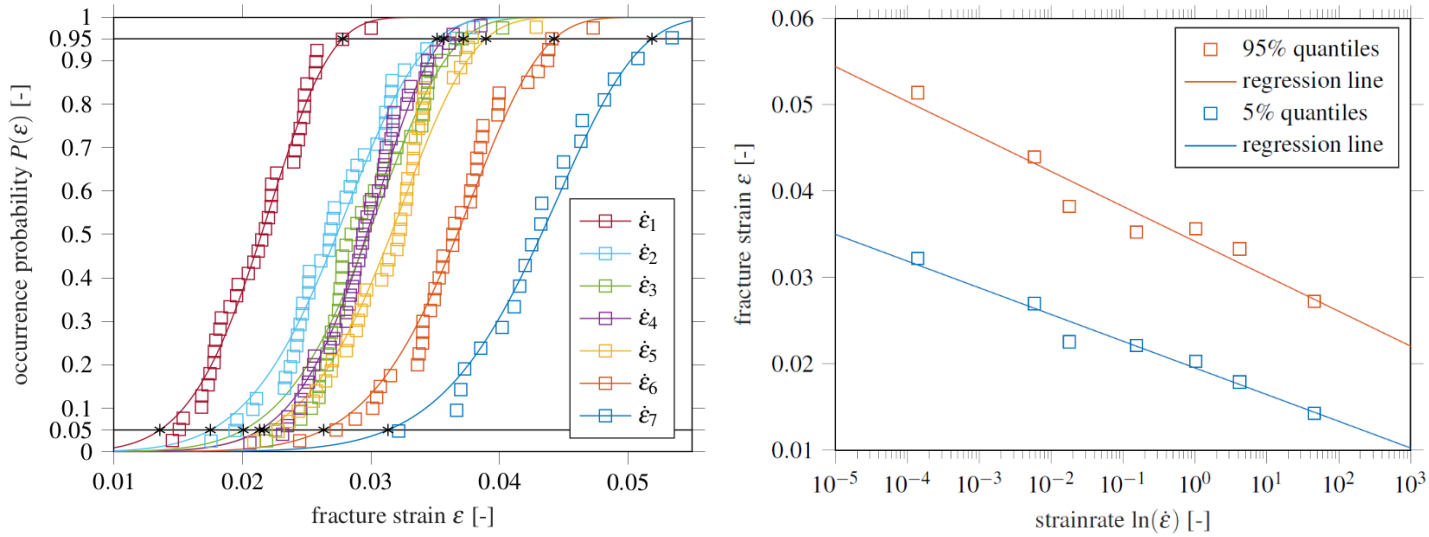

Figure 8 – Fracture strain distribution for seven different strain rates and the progression of their 5 % and 95 % quantiles

Here starts the modelling of the stochastic behaviour. As illustrated in Figure 8 the 5 % and the 95 % quantiles are taken from each of the seven CDFs. These are the strains at which statistically 5 % and analogously 95 % of the specimens have failed. Plotted over the logarithmic strain rate at the point of failure, we gain the diagram on the right side of Figure 8. The quantiles trend to a linear progression. In our statistic model, we introduce is the linear regression of these quantiles, i.e.

$$\varepsilon_{0.05} = f(\dot{\varepsilon}) \text{ , and} \quad (5)$$

$$\varepsilon_{0.95} = f(\dot{\varepsilon}) \text{ .} \quad (6)$$

Thus, by given strain rate we can predict the 5 % and the 95 % quantile. The two rate dependent parameters of the Weibull distribution can be solved by the following system of equations:

$$\left| \begin{array}{l} 0.05 = 1 - \exp\left[-\left(\frac{\varepsilon_{0.05}}{\eta}\right)^{\beta}\right] \\ 0.95 = 1 - \exp\left[-\left(\frac{\varepsilon_{0.95}}{\eta}\right)^{\beta}\right] \end{array} \right| \quad (7)$$

For β and η, the respective Weibull distribution is fully defined. Hence, for any given strain rate the fracture strain is predictable with a distinct occurrence probability. The model is visualized as surface plot on the right-hand side of Figure 9. In order to examine its quality, distribution functions are modelled for the strain rates from Table 1. On the left-hand side of Figure 9 these modelled distributions, visualized as solid lines, are compared to the empirical distribution of the experiments, marked as squares.

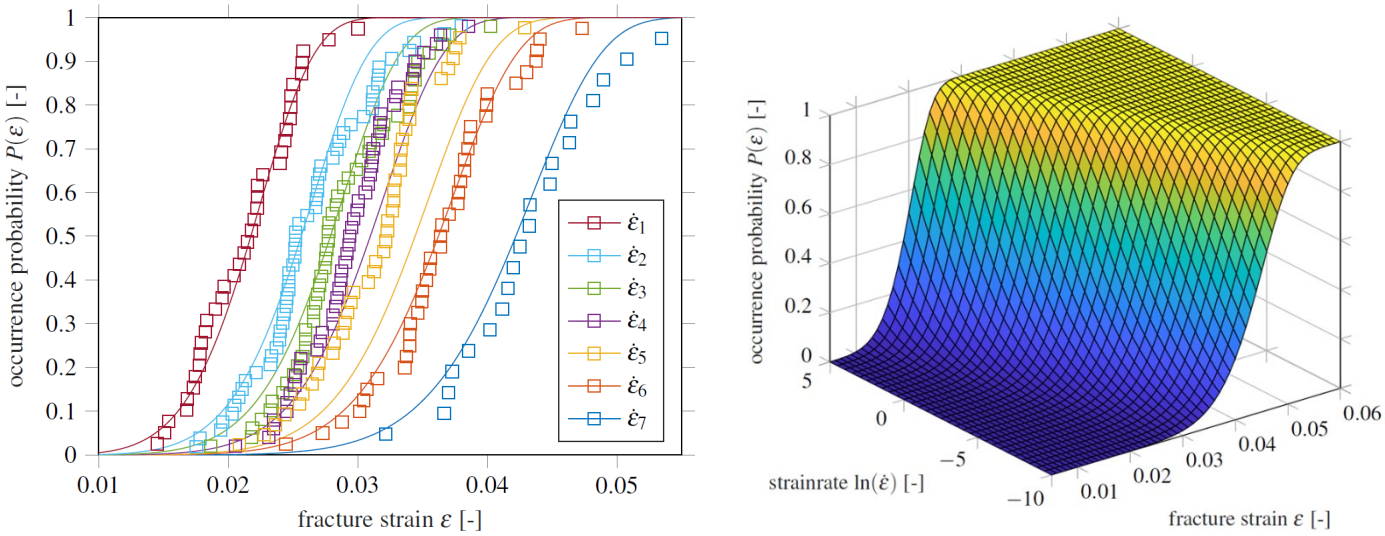

Figure 9 – Modeled fracture strain distributions (solid lines) compared to experiments (squares) and surface plot of the model

Evaluated optically, the empirical data is well reproduced with small offsets of the CDF, resulting from the unavoidable deviation of the quantile regression model shown in Figure 8. To quantify the quality of the fit, for each CDF the coefficient of determination is determined by

$$R^2 = 1 - \frac{\sum[p_i - P(\varepsilon_i)]^2}{\sum(p_i - \bar{p})^2}. \quad (8)$$

The R^2 value is a quantity for the deviation of function to data points. A R^2 in the magnitude of one is a good agreement, where a R^2 in the magnitude of zero is an indicator for no correspondence of function and data points. In Table 2 the results for the initial function fit are compared to the results of the quantile model for each strain rate. Except for the strain rate $\dot{\varepsilon}_5$ the coefficients of determination gain high scores which defines a good basis for the step towards stochastic simulation.

Table 2 – Coefficients of determination

Reference	Original Fit	Quantile Modelled
$\dot{\varepsilon}_1$	0.9819	0.9785
$\dot{\varepsilon}_2$	0.9622	0.9575
$\dot{\varepsilon}_3$	0.9461	0.9402
$\dot{\varepsilon}_4$	0.9874	0.8554
$\dot{\varepsilon}_5$	0.9784	0.5316
$\dot{\varepsilon}_6$	0.9780	0.9766
$\dot{\varepsilon}_7$	0.9846	0.9513
Mean:	0.9741	0.8844

Stochastic Simulation

Using the quantile model from the previous section, the occurrence probability for a fracture strain is described by the function

$$P(\varepsilon, \dot{\varepsilon}) = 1 - \exp\left[-\left(\frac{\varepsilon}{\eta(\dot{\varepsilon})}\right)^{\beta(\dot{\varepsilon})}\right]. \quad (9)$$

With respect to finite-element simulation, the model is changed for the requirements of the *MAT_ADD_EROSION environment. Equation (9) is solved for the fracture strain, leading to the approach

$$\varepsilon(P, \dot{\varepsilon}) = \eta(\dot{\varepsilon})\,[-\ln(1-P)]^{1/\beta(\dot{\varepsilon})}\,. \quad (10)$$

Now, for representative strain rates from 10^{-5} 1/s to 10^{2} 1/s, an erosion card is generated for a given probability P [10]. One might use this approach to check distinct occurrence probabilities, e.g. the 99 % quantile. But the model also enables stochastic simulations. For that, the value of P is provided by a random number generator, producing uniformly distributed numbers from zero to one. Meaning, N random probabilities P lead to N *MAT_ADD_EROSION cards for N repetitions of the simulation.

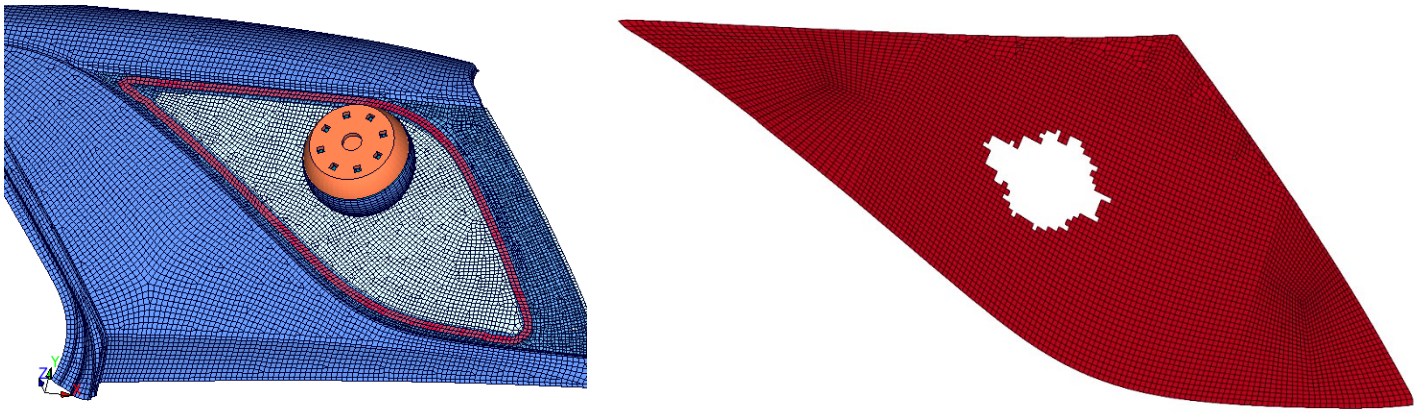

Figure 10 – Head impact model from [3] and fracture pattern of the side window adopted for stochastic simulation

The results of a varying fracture strain are examined for a head impact test, whose simulation model is adopted from [4]. As secondary quantity the head injury criterion (HIC) is considered, which is calculated from the resultant acceleration [g] of the head impactor by

$$HIC = \max\left\{\left[\frac{1}{t_2-t_1}\int_{t_1}^{t_2} a(t)\mathrm{d}t\right]^{2.5}(t_2-t_1)\right\}, \quad (11)$$

where the time interval is chosen to maximize the outcome, see [11]. For the test in Figure 5 the HIC interval is visualized in Figure 11. A common threshold to avoid serious damages of the head is HIC=1000, basing on medical research.

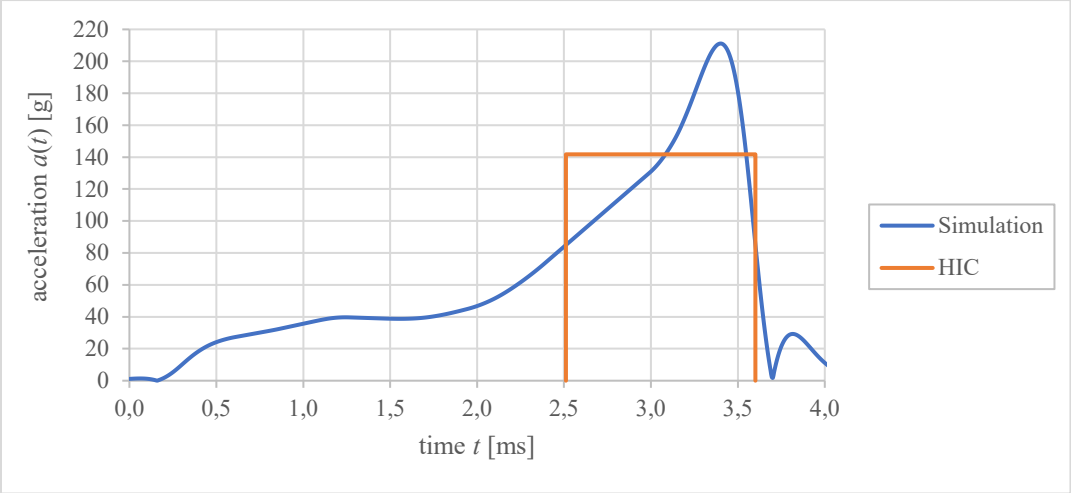

Figure 11 – Resultant acceleration of the head impactor from simulation and the interval for the HIC

The stochastic simulation of the head impact test in LS-DYNA is repeated 500 times, i.e. $N = 500$, resulting in 500 head injury criteria. The histogram in Figure 12 shows a skewed distribution for the occurred HIC values. Like the experimental fracture strains, the HICs are sorted ascendingly. Using Equation (2) for each HIC value an occurrence probability is assigned, giving the empirical distribution function in the right diagram of Figure 12.

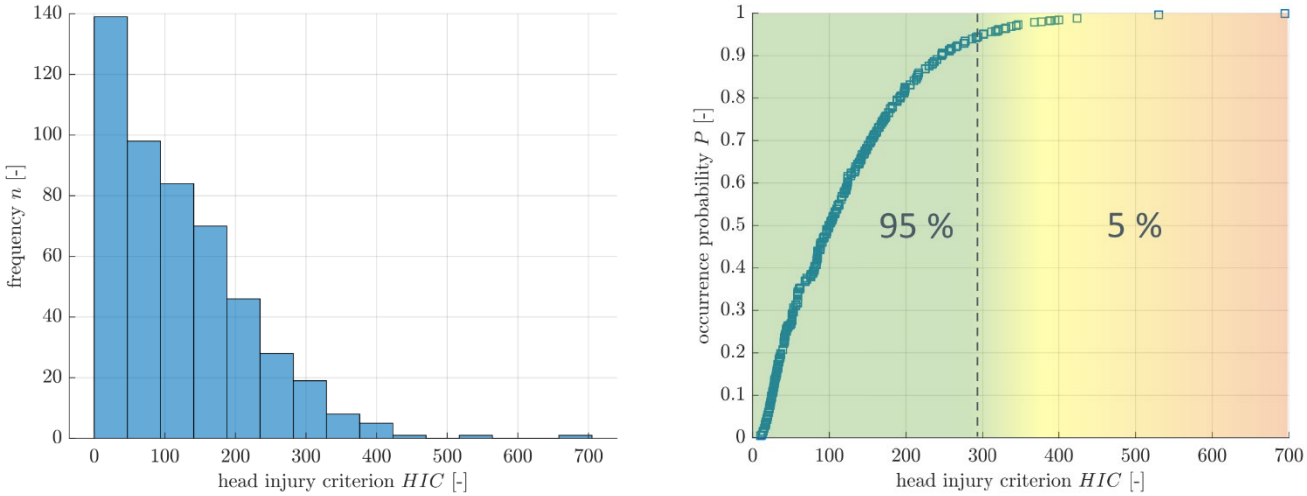

Figure 12 – HIC values of 500 head impact simulations with random fracture strains

Besides the skewness of the stochastic sample, the magnitude of the HIC spreads in an enormous range. For the experiment in Figure 5, the HIC is determined to 121, which is about the mean value of the simulated HICs. But in these 500 repetitions we also see one configuration leading to a HIC of nearly 700. With the threshold of 1000 in mind, that already enters a critical level. The relevance for safety evaluations of structural parts is evident: for a material with high variation in its fracture behaviour, a single experimental evaluation test carries the danger of underestimation of the risk potential. For instance, at volume production of automotive side windows it is most likely to have single units showing critically high HICs. We recommend the careful consideration, whether a statistical characterization of a materials failure interval would be a gain in application safety. With knowledge of the probability distribution a threshold interval, for example 95 % of the expected occurrences, should then be the evaluation benchmark.

Summary

In this work, we establish an approach for adding stochastic failure to *MAT_ADD_EROSION in LS-DYNA. Using an acrylic glass, an extensive experimental work is conducted in order to generate adequate sample sizes for statistical analyses, arising from seven different strain rates for the examination of the strain-rate dependent material behaviour. A very robust quantile regression model is introduced that is capable of delivering a probability distribution function for fracture strain in dependence on the strain rate. The integration of this model into stochastic simulation is demonstrated on head impact tests. For the head injury criterion, the importance of statistical evaluation methods is shown. A single evaluation test of a structural part might lead to false decisions for a design, since even small variations in the material behaviour can result in high deflection of the evaluation criterion.

References

[1] Rühl, A., Kolling, S., Schneider, J.: Characterization and modeling of poly(methyl methacrylate) and thermoplastic polyurethane for the application in laminated setups. Mech. Mat., 113 (2017), pp. 102–111.
[2] Rühl, A.: On the time and temperature dependent behaviour of laminated amorphous polymers subjected to low-velocity impact, Ph.D. thesis, (2017).
[3] Rühl, A., Kolling, S., Schneider, J.: A transparent three-layered laminate composed of poly(methyl methacrylate) and thermoplastic polyurethane subjected to low-velocity impact. Int. J. Impact Eng., 136 (2019), in press.
[4] Lopez Ruiz, D., Rühl, A., Kolling, S., Ruban, E., Kiesewetter, B., Ulzheimer, S.: CAE validation study of a side window impact using Plexiglas materials. Proceedings of the 10th European LS-DYNA Conference (2015).
[5] Ballarini, R., Pisano, G., and Royer-Carfagni, G.: The lower bound for glass strength and its interpretation with generalized Weibull statistics for structural applications. J. Eng. Mech., 142(12) (2016) 04016100.
[6] W.Weibull, A statistical theory of the strength of materials, Ing. Vet. Ak. Handl. 151 (1939).
[7] Makkonen, L.: Problems in the extreme value analysis. Struct. Saf. 30 (2008), pp. 405–419.
[8] T. W. Anderson, D. A. Darling, A test of goodness of fit, J. Am. Stat. Assoc. 49 (1954), pp. 765–769.
[9] Datsiou, K. C., Overend, M.: Weibull parameter estimation and goodness-of-fit for glass strength data. Struct. Saf. 73 (2018), pp. 29–41.
[10] Berlinger, M., Schrader, P., Kolling, S.: Analyses on the strain-rate dependent fracture behaviour of PMMA for stochastic simulations. Proceedings of the 15th LS-DYNA Forum (2018).
[11] Alter, C., Kolling, S., Schneider, J.: An enhanced non-local failure criterion for laminated glass under low velocity impact. Int. J. Impact Eng., 109 (2019), pp. 342–353.